

Efficient Radiolabeling of Block Copolymer Micelles through Radiometal Salt Precipitation for Theranostic Applications

Liu, Huanhuan; de Kruijff, Robin M.; Laan, Adrianus C.; Beekman, Freek J.; van den Heuvel, Eline; Ramakers, Ruud M.; Eelkema, Rienk; Denkova, Antonia G.

DOI

[10.1002/adtp.202200077](https://doi.org/10.1002/adtp.202200077)

Publication date

2022

Document Version

Final published version

Published in

Advanced Therapeutics

Citation (APA)

Liu, H., de Kruijff, R. M., Laan, A. C., Beekman, F. J., van den Heuvel, E., Ramakers, R. M., Eelkema, R., & Denkova, A. G. (2022). Efficient Radiolabeling of Block Copolymer Micelles through Radiometal Salt Precipitation for Theranostic Applications. *Advanced Therapeutics*, 5(9), Article 2200077. <https://doi.org/10.1002/adtp.202200077>

Important note

To cite this publication, please use the final published version (if applicable). Please check the document version above.

Copyright

Other than for strictly personal use, it is not permitted to download, forward or distribute the text or part of it, without the consent of the author(s) and/or copyright holder(s), unless the work is under an open content license such as Creative Commons.

Takedown policy

Please contact us and provide details if you believe this document breaches copyrights. We will remove access to the work immediately and investigate your claim.

Efficient Radiolabeling of Block Copolymer Micelles through Radiometal Salt Precipitation for Theranostic Applications

Huanhuan Liu, Robin M. de Kruijff, Adrianus C. Laan, Freek J. Beekman, Eline van den Heuvel, Ruud M. Ramakers, Rienk Eelkema, and Antonia G. Denkova*

A variety of polymer micelles are designed for the delivery of chemotherapeutic drugs to tumors. Although the promise of these nanocarriers is very high, in the clinic the effectivity is rather limited. Determining the in vivo fate of the micelles can greatly help to improve this treatment. Here, a simple and fast chelator-free method for radiolabeling of polymer micelles composed of different block copolymers is presented, which can allow evaluating the behavior of the nanocarriers in vivo using noninvasive nuclear imaging techniques (e.g., single photon computed tomography, SPECT). The radiolabeling method consists of adding the radioisotope ions, i.e., $^{111}\text{In(III)}$, resulting in a high radiolabeling efficiencies up to 90%. The results suggest that the radiolabeling efficiency depends on two important factors: the properties of the hydrophobic block in the block copolymer composing the micelle core, and the speciation of the radiometal salts. The formation of metal hydroxides and their precipitation in the core of the micelles appears to be a key factor for high stability. Moreover, the method can be applied to radiolabel the micelles in the presence of chemotherapeutic drugs. Finally, a SPECT study shows that the radiolabeled samples are stable in vivo without any evident loss of $^{111}\text{In(III)}$.

for chemotherapy, leading to several formulations that are currently clinically applied.^[2] Micelles have a typical core-shell structure, the hydrophobic core is used to encapsulate water-insoluble substances and the hydrophilic shell reduces interaction with plasma proteins.^[3] The application of polymer micelles in drug delivery to tumors relies on the so-called enhanced permeability and retention (EPR) effect. The EPR, however, seems to vary among different patients and cancer types and therefore micelle formulation appears often to be less efficient when translated to the clinic.^[4] Besides this, there are other factors, such as the leakage of the encapsulated drugs and accumulation in healthy tissue, that influence the effectivity of a nanocarrier.^[2] In order to understand and to improve the application of polymer micelles in chemotherapy, it is important to determine their biodistribution and pharmacokinetics prior or during actual application.


Imaging techniques, such as single photon emission computed tomography (SPECT) and positron emission tomography (PET), are powerful tools for tracing and evaluating the in vivo performance of nanocarriers in both preclinical setting as well as in the clinic.^[5,6] In order to use either PET or SPECT, the micelles need to be radiolabeled. For this purpose, chelators which are capable of forming strong metal ion complexes with the radiometals are typically conjugated to the outer surface of the micelles.^[5-7] Poly(ethylene

1. Introduction

In the last two decades, nanotechnology has shown great potential in the field of medicine. A variety of nanosized vehicles with different compositions, morphologies, and properties have been developed primarily to ensure safer and more effective drug delivery processes.^[1] Among these different nanocarriers, polymer micelles have shown to be among the most promising candidates

H. Liu, R. M. de Kruijff, A. C. Laan, F. J. Beekman, E. van den Heuvel, R. M. Ramakers
Department of Radiation Science and Technology
Delft University of Technology
Mekelweg 15, Delft 2629 JB, The Netherlands

F. J. Beekman, R. M. Ramakers
MILabs B.V.
Heidelberglaan 100, Utrecht 3584 CX, The Netherlands
F. J. Beekman, R. M. Ramakers
Department of Translational Neuroscience, Brain Center Rudolf Magnus
University Medical Center Utrecht
Lundlaan, Utrecht 3584, The Netherlands
R. Eelkema
Department of Chemical Engineering
Delft University of Technology
Delft 2629 HZ, The Netherlands
A. G. Denkova
Department of Radiation Science and Technology
Delft University of Technology
Delft 2629 JB, The Netherlands
E-mail: a.g.denkova@tudelft.nl

 The ORCID identification number(s) for the author(s) of this article can be found under <https://doi.org/10.1002/adtp.202200077>

© 2022 The Authors. *Advanced Therapeutics* published by Wiley-VCH GmbH. This is an open access article under the terms of the Creative Commons Attribution-NonCommercial License, which permits use, distribution and reproduction in any medium, provided the original work is properly cited and is not used for commercial purposes.

DOI: 10.1002/adtp.202200077

glycol (PEG), also referred to as poly(ethylene oxide) (PEO), is usually selected as the hydrophilic shell material to decrease contact with blood proteins and therefore increase the in vivo circulation of micelles. However, several studies have demonstrated that a slight change in surface properties can significantly influence the in vivo performance of nanocarriers such as blood circulation and biodistribution.^[8,9] Therefore, micelle modification requires judicious design to maintain the desired behavior of the micelles. Moreover, chelator based radiolabeling implies additional synthesis steps such as conjugation of ligands to the block copolymer, which increases the complexity of the formulation.^[10] Thus, radiolabeling methods without chelators are desirable.^[11]

In this work, we present an easy, fast, and chelator-free method for radiolabeling the core of polymer micelles and we provide insights into the mechanism of this process. For this purpose, we have selected several block copolymers with PEO-based hydrophilic blocks, i.e., poly(caprolactone-*b*-ethylene oxide) (including PCL-PEO (2800–2000), PCL-PEO (6500–5500), PCL-PEO (10 000–5000), and PCL-PEO (13 000–5000)), poly(lactic acid-*b*-ethylene oxide) (PLA-PEO (10 500–5000)), poly(butadiene-*b*-ethylene oxide) (PBd-PEO (5500–5000)), and poly(styrene-*b*-ethylene oxide) (PS-PEO (9500–18 000)). Using these polymers, we prepared micelles, radiolabeled them with ¹¹¹In(III), and compared their radiolabeling efficiency and stability. We used cryogenic electron microscope (Cryo-EM) and Fourier-transform infrared spectroscopy (FT-IR) to get insight into the interaction mechanism between the metal ions and the polymer micelles, and the subsequently developed hypothesis was checked using another radioisotope, i.e., ¹⁷⁷Lu(III). Finally, to establish the practical application of this method, we showed that the radiolabeling method can be carried out in the presence of chemotherapeutic drugs such as paclitaxel (PTX). Moreover, we also investigated the in vivo stability of the radiolabeled micelles using SPECT/CT.

2. Results and Discussion

2.1. Radiolabeling of Different Type of Micelles with ¹¹¹In (III)

Using the solvent-evaporation method, we made polymer micelles from several types of PEO-based block copolymers, including four PCL-PEO variants, namely, PCL-2800, PCL-6500, PCL-10000, and PCL-13000, and PLA, PBd, and PS block copolymers. Figure S1 in the Supporting Information shows dynamic light scattering (DLS) and Cryo-EM describing the size distribution and morphology of the PCL-PEO micelles as-prepared without filtration. According to DLS data, the mean hydrodynamic radius of PCL-2800, PCL-6500, PCL-10000, and PCL-13000 micelles, was ≈ 16 , 39, 54, and 65 nm, respectively. The Cryo-EM images indicated that the polymers with shorter chain preferably formed small spherical micelles while the longer PCL chain polymers resulted in larger spherical structures that appear to be less dense than the smaller micelles. As for the micelles composed by the other block copolymers, the mean hydrodynamic radius was ≈ 85 , 96, and 56 nm for PLA, PBd, and PS micelles, respectively. In some of the samples, larger aggregates could be observed. The larger aggregates were removed by syringe filtration prior to the radiolabeling procedure.^[12]

The radioisotope ¹¹¹In(III) is typically used in SPECT imaging due to its gamma energies of 171.3 and 245.4 keV which are

suitable for imaging, as well as its favorable half-life ($t_{1/2} = 2.8$ days).^[13] In this work, we attempted to radiolabel different polymer micelles by simply adding ¹¹¹In(III) solution to the micelles followed by a 30 min incubation time. The process was terminated by removing the nonencapsulated ¹¹¹In(III) from the micelles using size exclusion chromatography (SEC). All PCL-PEO micelles could be radiolabeled using this method, yielding radiolabeling efficiencies of $81.9 \pm 1.6\%$, $83.8 \pm 1.5\%$, $92.4 \pm 2.4\%$, and $90.7 \pm 3.2\%$ for PCL-2800, PCL-6500, PCL-10000, and PCL-13000 micelles, respectively. In contrast, the other block copolymer micelles showed relatively lower uptake of ¹¹¹In (III), resulting in a radiolabeling efficiency of $69.7 \pm 3.3\%$, $56.5 \pm 6.8\%$, and $16.1 \pm 2.6\%$ for PLA micelles, PBd-micelles, and PS-micelles, respectively (Figure 1).

To test the radiolabeling stability, we used an excess of the chelator diethylene triamine pentaacetic acid (DTPA) which is known to have a high affinity for indium ions.^[14] Figure 1b shows the In fraction that remained in the micelles upon incubation with DTPA for 24 h. Clearly, PCL- and PLA-based micelles had much better radiolabeling stability than the PS or PBd micelles, in which only around 20% of ¹¹¹In(III) remained encapsulated after the DTPA challenge.

2.2. Interaction Mechanism between Indium Species and Micelles

The initial ¹¹¹In(III) activity used in the loading and retention experiments was 50 kBq, which resulted in a final In(III) concentration of $\approx 2.9 \times 10^{-11}$ M in the sample. This concentration was too low for investigating the mechanism of interaction between the In species and the micelles. Therefore, we increased the In(III) concentration to 0.137×10^{-3} M by using nonradioactive InCl₃. In some of the experiments, we did use ¹¹¹In(III) as a radiotracer to enable easy evaluation of the loading efficiency. Although all PCL-PEO micelles displayed a high radiolabeling efficiency when using 50 kBq of ¹¹¹In(III), the loading performance differed when the concentration of InCl₃ (Table S1, Supporting Information) was increased. The larger micelles, i.e., PCL-10000 and PCL-13000, could encapsulate more In(III), particularly the PCL-10000 micelles which exhibited a loading efficiency of $50.8 \pm 1.8\%$. In contrast, PCL-2800 and PCL-6500 displayed a loading efficiency of just $3.9 \pm 0.1\%$ and $4.3 \pm 0.1\%$, respectively. Nevertheless, considering the relatively high indium concentration, a large amount of In(III) could still be encapsulated in all PCL-PEO micelles. Naturally, higher concentrations should lead to lower encapsulation efficiencies.

We used Cryo-EM to study the interaction between PCL-10000 micelles and In(III) solution prepared by dissolving InCl₃ in HCl aqueous solution with a pH 2. The samples for Cryo-EM were prepared by plunge-freezing the micelles-indium mixture in liquid ethane after a reaction time of 2, 10, or 30 min, without separation of the free indium ions. The introduction of In(III) solution led to the appearance of dark spots in the samples (Figure 2b–h), which could not be found in the images of the empty micelles (see Figure 2a). After 2 min of reaction, the majority of the indium nanoparticles (yellow arrows in Figure 2) were still outside the micelles (red circles). When the reaction time reached 10 min, the indium aggregation outside the micelles decreased (Figure

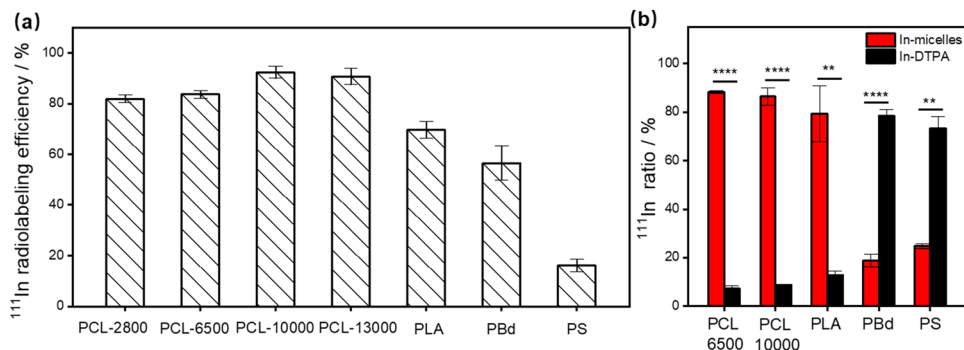


Figure 1. a) The $^{111}\text{In}(\text{III})$ radiolabeling efficiency of polymer micelles composed of different PEO-derived block copolymers (polymer concentration: 4.3 mg mL^{-1} for PCL/PBd/PS micelles and 2.5 mg mL^{-1} for PLA micelles, in $10 \times 10^{-3} \text{ M}$ HEPES buffer with $\text{pH} = 7.4$); b) the $^{111}\text{In}(\text{III})$ radiolabeling stability of micelles challenged with DTPA for 24 h. DTPA concentration: $1 \times 10^{-3} \text{ M}$, in $10 \times 10^{-3} \text{ M}$ HEPES buffer with $\text{pH} = 7.4$; polymer concentration: $\approx 0.79 \text{ mg mL}^{-1}$ for PCL/PBd/PS micelles and $\approx 0.45 \text{ mg mL}^{-1}$ for PLA micelles. The data are presented as mean \pm SD, standard deviation based on three separate experiments. Student's *t*-test has been applied for the comparison between two groups. $**p \leq 0.01$ and $****p \leq 0.0001$ represent significance between the activity remaining in the micelles and or bound to DTPA.

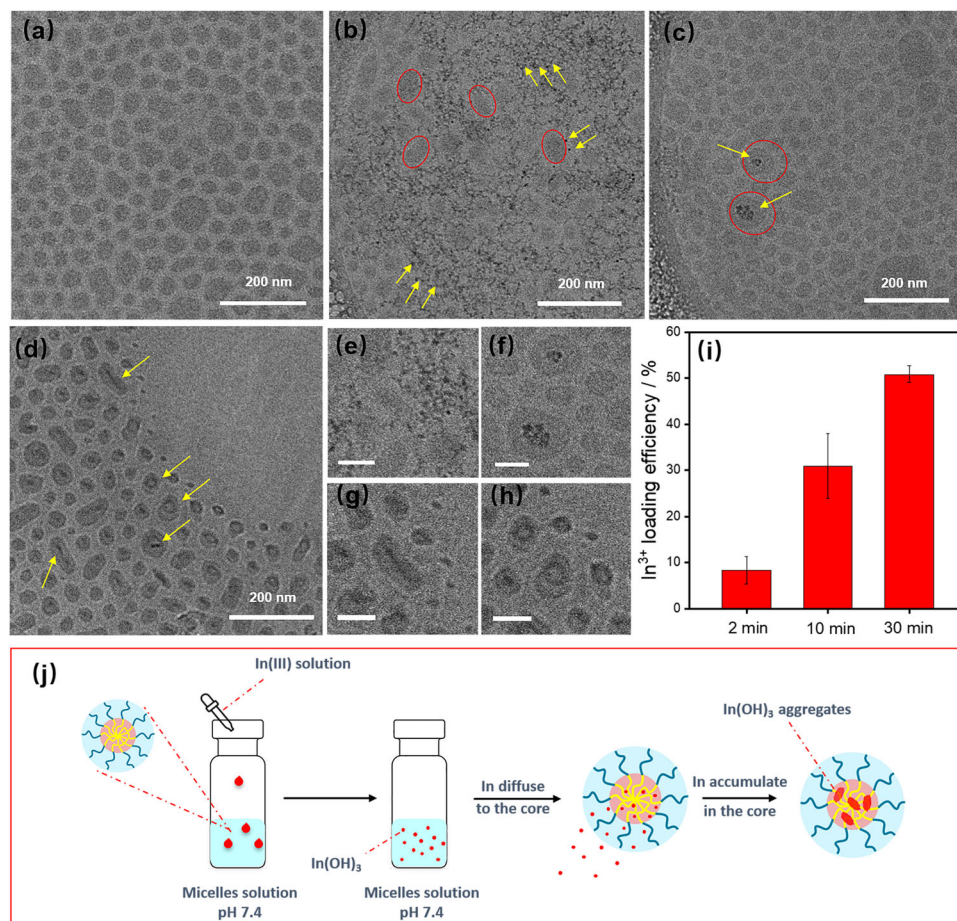


Figure 2. Cryo-EM of a) empty PCL-10000 micelles, and mixture of $\text{In}(\text{III})$ species and PCL-10000 micelles obtained after reacting for b) 2, c) 10, and d) 30 min; the enlarged image for samples obtained after reacting for e) 2, f) 10, and g, h) 30 min (the scale bar in (e–h) represents 50 nm); yellow arrows in (a–d) point at nanoparticle structures. i) The $\text{In}(\text{III})$ loading efficiency of PCL-10000 micelles after interacting with ^{111}In radiolabeled ions for different times: 2, 10, and 30 min. (The data are presented as mean \pm SD, standard deviation based on three separate experiments.) The concentration of the polymer was 4.3 mg mL^{-1} in HEPES buffer and the initial $\text{In}(\text{III})$ concentration was $0.137 \times 10^{-3} \text{ M}$. j) Proposed formation process of $\text{In}(\text{III})$ -loaded PCL-PEO micelles.

S4, Supporting Information), and the dark spots started to appear inside the micelles (see Figure 2c) with most of the micelles still being empty. After 30 min, clear dark spots could be observed in the majority of the micelles (Figure 2d). The encapsulated In nanoparticles had at that point various shapes, such as rods and tori (as shown in Figure 2g,h), which differed from the ones in Figure 2b,e where mostly spherical nanoparticles were found.

Next, we measured the loading efficiency of In species in PCL-10000 micelles as function of time by using In(III) solution mixed with radioactive $^{111}\text{In(III)}$ functioning as a tracer. Here, we used SEC to separate the free In(III) from the micelle fraction after reacting for 2, 10, and 30 min. The results (Figure 2i) showed that $8.7 \pm 3.0\%$ of In(III) was already loaded in the micelles after 2 min, which increased to 30.9% after 10 min and 50.8% after 30 min. The increasing loading efficiency as function of time shows that the transport of In species into the PCL-PEO micelles is a time-dependent process.

To further look into the mechanism of interaction between In species and micelles, we also did a control experiment by adding the In(III) to a solution in the absence of micelles. Within 3 min, precipitates could be clearly observed on the wall of the glass vial, while the vial containing PCL-PEO micelles did not show any precipitation observable by eye. According to CHEAQS, a metal speciation calculation program,^[15] and as reported in the literature, the precipitate is expected to be In(OH)_3 , which forms spontaneously by hydrolysis of indium chloride.^[16] The observed phenomena indicate that indium ions tend to form insoluble hydroxides once being introduced into the 4-(2-hydroxyethyl)-1-piperazineethanesulfonic acid (HEPES) buffer at neutral pH, and the subsequent interaction between the micelles and the indium species limits or even eliminates the self-aggregation of the insoluble indium species outside the micelles. Moreover, considering the relatively fast formation of indium hydroxides, it is most likely that In(III) would react with the micelles in the form of indium hydroxides.

As shown in Figure 2a–h, once being added to the micelle solution, In species are formed outside the micelles, which gradually enter the hydrophobic core of the micelles. We propose the radiolabeling mechanism to occur as follow: the addition of indium chloride solution to the aqueous solution leads to the formation of soluble In-hydroxides which can enter the core of the micelles, and with the increasing accumulation of In(III) in the hydrophobic core, solid In(OH)_3 forms, see Figure 2j. Speciation calculations using CHEAQS (shown in Figure S3a,b, Supporting Information) support this theory. The driving force leading to the accumulation of In species in the polymeric core, however, remains unknown. In the case of the loading process using non-radioactive indium, which has a relatively high In concentration, we cannot fully eliminate the possibility that solid In(OH)_3 precipitates are formed first and as such diffuse into the core of the micelles.

The inherent properties of the polymers play an important role in the radiolabeling process. The presence of carbonyl groups in the hydrophobic part of PCL-PEO and PLA-PEO polymer can form hydrogen bonds with water molecules, which leads to slight hydrophilicity.^[17] Contrarily, polybutadiene and polystyrene are known to be very hydrophobic and much less permeable than PLA or PCL.^[18,19] The highly hydrophobic cores of PS and PB block copolymers will form a sharp interface and limit the con-

tact between water and the core polymer.^[20] Assuming that water is essential for the diffusion of indium species into the core, the less water content there is in the core, the less In species would be found inside the micelles. Moreover, FT-IR experiments (Figure S5, Supporting Information) show that there is no change in the IR spectrum of the polymer core upon In encapsulation, suggesting that there is no chemical interaction between In species and the polymers. These results suggest that the hydrophobic nature of the polymers is the limiting factor. Furthermore, the radiolabeling data show that to achieve good stability a high enough In(III) concentration should be reached in the core, probably leading to precipitates.

2.3. Radiolabeling of PCL-PEO Micelles with $^{177}\text{Lu(III)}$

To get further insight into the radiolabeling mechanism, we attempted to radiolabel PCL micelles with another radioisotope. $^{177}\text{Lu(III)}$ was chosen since it is typically used in radionuclide therapy.^[21,22] The radiolabeling results showed that PCL-6500 micelles have excellent radiolabeling efficiency for $^{177}\text{Lu(III)}$ achieving up to $94.2 \pm 0.5\%$, which is comparable to that of $^{111}\text{In(III)}$ ($83.8 \pm 1.5\%$). However, the radiolabeling stability differed significantly. The $^{111}\text{In(III)}$ radiolabeled micelles showed the best stability, with only $7.3 \pm 1.4\%$ of the encapsulated $^{111}\text{In(III)}$ removed from the micelles by DTPA. In contrast, the $^{177}\text{Lu(III)}$ radiolabeled samples showed that $78.4 \pm 0.3\%$ of $^{177}\text{Lu(III)}$ was lost from the PCL-6500 micelles in the presence of DTPA, indicating a poor stability.

To better understand the radiolabeling mechanism, we employed CHEAQS again to simulate the speciation of the lutetium ions. Lutetium shows complex speciation as function of pH and concentration (Figure S3c,d, Supporting Information). Under lower concentration, i.e., $5.71 \times 10^{-10} \text{ M}$ (50 kBq), free Lu^{3+} ions are the major species under acidic conditions, while Lu(OH)_4^- ions are mainly formed in alkaline environment. The percentage of aqueous Lu(OH)_3 increases to a maximum around pH 8 but it is still not the dominant species under these conditions. Besides, solid Lu(OH)_3 starts to appear at concentrations of Lu^{3+} above $1 \times 10^{-8} \text{ M}$ in a solution with a pH value of 8.

Although CHEAQS predicts the formation of a low percentage of Lu-hydroxides under our experimental conditions ($10 \times 10^{-3} \text{ M}$ HEPES buffer, pH 7.4; $[\text{Lu}^{3+}] = 5.71 \times 10^{-10} \text{ M}$), we suspect that they do contribute to a high radiolabeling efficiency. To test this hypothesis, we performed radiolabeling experiments at pH 2 where lutetium is mostly present as free Lu^{3+} ions. The results showed a very low radiolabeling efficiency ($0.31 \pm 0.06\%$), suggesting that hydroxides are important for radiolabeling. Furthermore, we checked our assumption that precipitation is required to have high labeling stability by adding nonradioactive Lu(III) to increase the Lu(III) concentration to $5 \times 10^{-6} \text{ M}$ and using a tiny amount of $^{177}\text{Lu(III)}$ as a radiotracer. At this concentration, CHEAQS predicts solid $\text{Lu(OH)}_{3(s)}$ as the major species (Figure S3d, Supporting Information). After reacting for 30 min, we obtained a Lu loading efficiency of $29.1 \pm 1.4\%$. As shown in Figure 3, the concentration increase resulted in much better stability, i.e., $81.7 \pm 5.9\%$ of Lu(III) remained in the micelles 24 h after DTPA challenge. At lower Lu(III) concentration, i.e., $5.71 \times 10^{-10} \text{ M}$, at least three times less Lu is retained in the micelles which

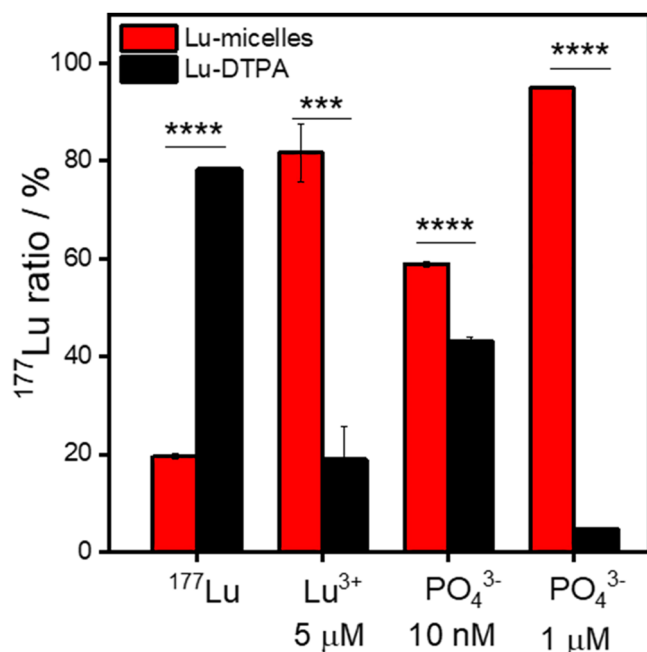


Figure 3. The $^{177}\text{Lu(III)}$ radiolabeling stability in DTPA solution for $^{177}\text{Lu(III)}$ radiolabeled PCL-6500 micelles prepared under different conditions. ^{177}Lu : adding 50 kBq of $^{177}\text{Lu(III)}$; Lu^{3+} 5×10^{-6} M: adding 5×10^{-6} M of nonradioactive Lu(III) during the radiolabeling process; PO_4^{3-} 10×10^{-9} M: adding 10×10^{-9} M sodium phosphate to the $^{177}\text{Lu(III)}$ labeled micelles and reacting for 1 h; PO_4^{3-} 1×10^{-6} M: adding 1×10^{-6} M sodium phosphate to the $^{177}\text{Lu(III)}$ labeled micelles and reacting for 1 h. (Polymer concentration: 4.3 mg mL^{-1} for radiolabeling and 0.79 mg mL^{-1} for DTPA test. The data points represent the mean \pm SD based on three separate experiments ($n = 3$). Student's t -test has been applied for the comparison between two groups. $***p \leq 0.001$ and $****p \leq 0.0001$ represent significance between the activity remaining in the micelles and when bound to DTPA.

clearly points to the role of precipitation. To further confirm the importance of precipitates, we also tried adding small amounts of phosphate ions, which according to CHEAQS should result in solid LuPO_4 , to the as-prepared $^{177}\text{Lu(III)}$ radiolabeled micelles. After 1 h of reaction, the DTPA test was carried out. Figure 3 shows that the addition of 10×10^{-9} M of PO_4^{3-} substantially increased stability and when increasing the concentration of PO_4^{3-} to 1×10^{-6} M, more than 90% of ^{177}Lu was retained inside the micelles after 1 day of incubation with DTPA.

2.4. $^{111}\text{In(III)}$ Radiolabeled PTX-Loaded Micelles

Next, we wanted to demonstrate that radiolabeling of the micelles could also be carried out in the presence of a chemotherapeutic drug. For this purpose, paclitaxel (PTX)-loaded micelles were prepared by adding PTX during the block copolymer micelles self-assembly process. The presence of the PTX drug did not significantly influence the size of the obtained micelles when using an initial mass ratio between PTX and polymers of 1:40 (Figure S6, Supporting Information). The loading efficiencies of the encapsulated PTX was determined by high-performance liquid chromatography (HPLC), showing a decrease with an increasing size of the micelles, i.e., $86.4 \pm 6.3\%$, $75.7 \pm 6.8\%$, and $63.4 \pm 7.3\%$ of

PTX were encapsulated by PCL-2800, PCL-6500, and PCL-10000 micelles, respectively. Subsequently, $^{111}\text{In(III)}$ was added to radiolabel the PTX-loaded micelles in the same way as used for the empty micelles. The radiolabeling efficiency was found to decrease slightly when compared to the empty micelles but it was sufficiently high (in all cases more than 60%) (Figure 4a).

We further checked the radiolabeling stability of the PTX-loaded micelles by the DTPA stability test and also in the presence of phosphate buffered saline (PBS, pH 7.4). As summarized in Figure 4b, the DTPA challenge showed that the co-loaded micelles displayed a good stability with more than 80% of the encapsulated $^{111}\text{In(III)}$ remaining inside the micelles, regardless of the block copolymer used. Besides, the three co-loaded samples exhibited excellent radiolabeling stability in PBS buffer with more than 80% of $^{111}\text{In(III)}$ remaining in the micelles after 1 day of incubation. We also compared the radiolabeling stability between PCL-6500 and PTX-loaded PCL-6500 micelles under DTPA challenging and serum test. The result in Figure 4c showed that the radiolabeling stability of PTX-loaded micelles was comparable with that of the empty PCL-6500 micelles, indicating the presence of PTX did not have significant influence on the interaction between ^{111}In and the micelles.

2.5. Stability In Vivo

Finally, we attempted to show the stability of radiolabeling as well as the imaging potential of the radiolabeled micelles, by performing preliminary pharmacokinetic studies using $^{111}\text{In(III)}$ radiolabeled PCL-6500 micelles. It has to be noted that the purpose of this study was not to determine the best conditions for in vivo delivery but to check the safety and utilization potential of this radiolabeling method. Therefore, we have chosen healthy mice for the in vivo studies. We radiolabeled the PCL-6500 micelles with $^{111}\text{In(III)}$, and achieved $\approx 66 \text{ MBq}$ of $^{111}\text{In(III)}$ encapsulated in the micelles when given an initial activity of 80 MBq. The $^{111}\text{In(III)}$ retention was found to be around 93% after being incubated with serum at 37 °C for 4 h.

The SPECT/CT results shown in Figure 5 indicate that the majority of activity appeared in the liver 1 h post-injection, and a small amount of $^{111}\text{In(III)}$ was found in the spleen. At the same time, the heart also contained radioactivity showing that the micelles were still circulating in the blood stream. For micelles and nanocarriers of this size, liver and spleen uptake is expected since they are the typical organs of the mononuclear phagocyte system.^[23–25] VOI (volume of interest) analysis was used to quantitatively analyze the activity distribution in different organs.^[26,27] The results showed that $56.4 \pm 6.2\%$ of the activity ended in the liver, $1.1 \pm 0.8\%$ activity was detected at the spleen, and $1.1 \pm 0.3\%$ of the activity was found in the heart 1 h post-injection. At 24 h post-injection, almost no activity could be observed in the heart. At the same time, $55.4 \pm 4.2\%$ and $1.9 \pm 0.4\%$ of the activity was detected in the liver and the spleen, respectively. At 48 h post-injection, the same activity values were measured in liver and spleen ($54.1 \pm 3.8\%$ and $2.0 \pm 0.8\%$, respectively) showing the $^{111}\text{In(III)}$ did not leach out of the micelles. The SPECT analysis thus shows that the radiolabeled micelles were stable in vivo. In addition, the mice did not exhibit any signs of discomfort after the experiments, which shows that the formulation was not toxic.

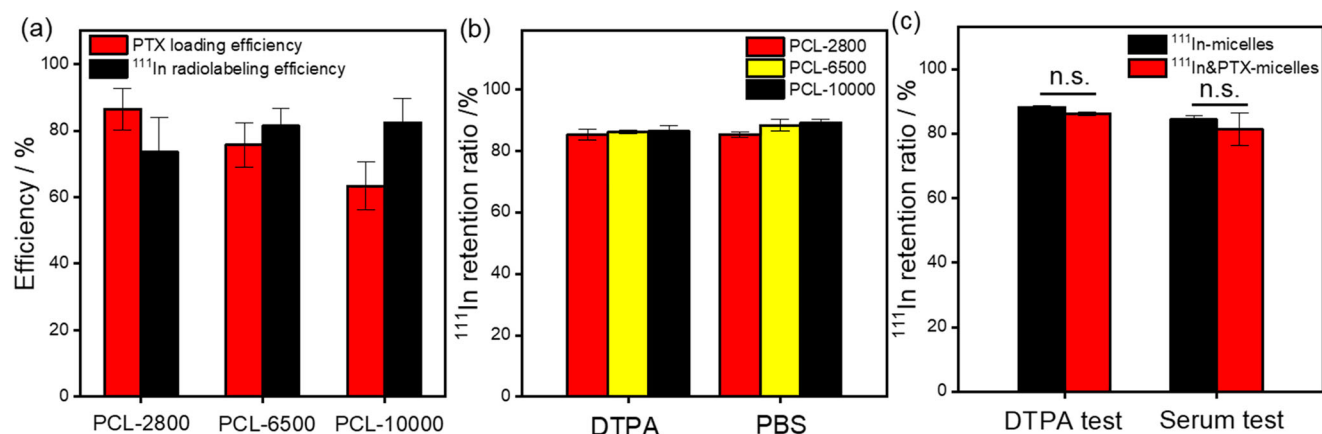


Figure 4. a) The PTX loading and ¹¹¹In(III) radiolabeling efficiency of ¹¹¹In&PTX co-loaded PCL-PEO micelles prepared with different block copolymers (data points represent the mean \pm SD ($n = 3$)); b) the radiolabeling stability of ¹¹¹In&PTX co-loaded PCL-PEO micelles after 24 h of incubation in PBS buffer (pH 7.4) and under DTPA test; c) comparison of the radiolabeling stability between ¹¹¹In radiolabeled PCL-6500 micelles and ¹¹¹In&PTX co-loaded PCL-6500 micelles under DTPA challenge and serum test. Polymer concentration: $\approx 0.79 \text{ mg mL}^{-1}$ for DTPA test and $\approx 0.44 \text{ mg mL}^{-1}$ for PBS test and serum test. The data points represent the mean \pm SD based on three separate experiments ($n = 3$). Student's *t*-test has been applied for the comparison between two groups. n.s. corresponds to "no significant" difference between ¹¹¹In-micelles and ¹¹¹In&PTX-micelles when challenged for 24 h by DTPA or when placed in serum.

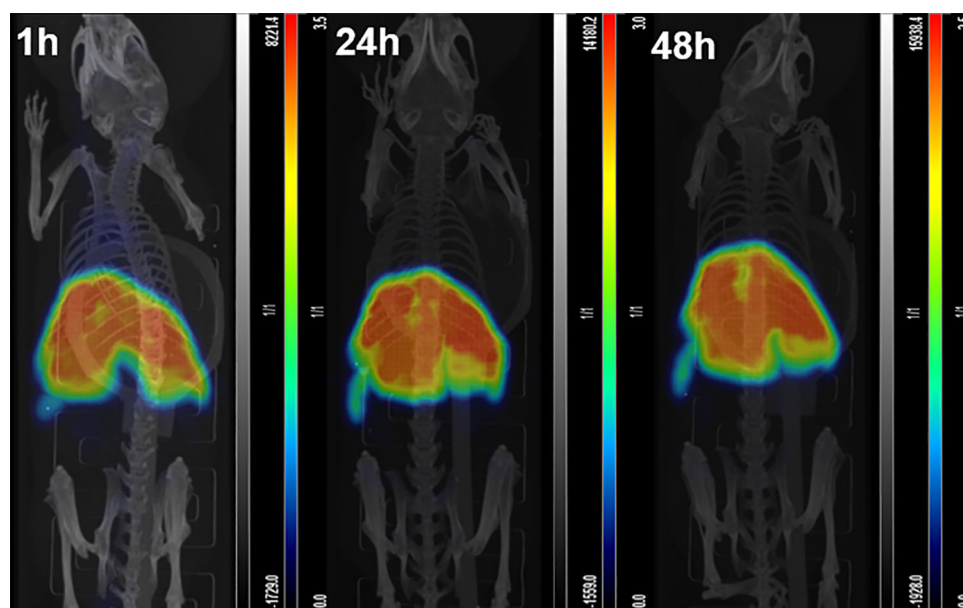


Figure 5. SPECT/CT images of ¹¹¹In(III) radiolabeled PCL-6500 micelles in healthy mice measured at 1, 24, and 48 h post-injection. The polymer concentration of the micelle solution in PBS was 4.3 mg mL^{-1} , the initially administered activity was around 10 MBq.

3. Conclusion

In this paper, we demonstrated a fast, easy, and chelator-free method to radiolabel block copolymer micelles. Different from conventional radiolabeling strategies which usually attach the isotopes on the surface of polymer micelles, this method radiolabels the hydrophobic core of the micelles, which can avoid unnecessary contact between the isotopes and proteins in the bloodstream. To achieve high radiolabeling efficiency, several conditions must be fulfilled. A first important factor is the nature of

the block copolymer composing the core, i.e., to obtain high radiolabeling yields the polymer should not be too hydrophobic. To achieve good radiolabeling stability, the metal species accumulated in the core of the micelles should form solid precipitates. Fulfilling these conditions enables efficient radiolabeling, also in the presence of a chemotherapeutic drug, combined with high *in vivo* stability of the radiolabeled particles.

The presented method here is not only extremely simple and straightforward, but it can be applied to common polymer micelles without any further modification while reaching high load-

ing efficiency. Therefore, we envision many new exciting applications, not only in nuclear medicine but also in various other fields where tracer particles are desired.

4. Experimental Section

Materials: The block copolymers poly(*ε*-caprolactone-*b*-ethylene oxide) (including PCL-PEO (2800–2000), PCL-PEO (6500–5500), PCL-PEO (10 000–5000), and PCL-PEO (13 000–5000)), poly(lactide-*b*-ethylene oxide) (PLA-PEO (10 500–5000)), poly(styrene-*b*-ethylene oxide) (PS-PEO (9500–18 000)), and poly(butadiene-*b*-ethylene oxide) (PBd-PEO (5500–5000)) were bought from Polymer Source (Quebec, Canada). Indium(III) chloride (InCl₃), HEPES, sodium phosphate (Na₃PO₄), paclitaxel (PTX), acetonitrile, Sephadex G-25 resins, Sepharose 4B gels, and Amicon Ultra-4 centrifugal filter were bought from Sigma Aldrich (Zwijndrecht, the Netherlands). HCl and Fetal bovine serum (FBS) was ordered from VWR International BV (Amsterdam, the Netherlands). ¹¹¹In and ¹⁷⁷Lu (in 0.01 M HCl solution, with a specific activity of 15.5 and 0.5 GBq μg⁻¹ for ¹¹¹In and ¹⁷⁷Lu, respectively) were kindly provided by Erasmus Medical Centre (Rotterdam, the Netherlands).

Synthesis of Polymer Micelles: The micelles were prepared by the solvent evaporation method described in previous publication.^[13] Typically, polymer stock solutions were prepared by dissolving PCL-PEO, PBd-PEO, or PS-PEO block copolymers (20 mg) in chloroform (0.2 mL). Then the mixture was added dropwise to 2.3 mL of Milli-Q (MQ) water and kept stirring overnight to remove the organic solvent. The PLA-PEO micelles were prepared in a slightly different way: PLA-PEO (20 mg) polymer was dissolved in acetonitrile (1.0 mL) and sonicated for 20 min to fully dissolve the polymer powder. Then, the mixture was added to MQ water (4.0 mL) followed by stirring overnight to remove the acetonitrile. After preparation, the obtained micelles were filtered through syringe filters (220 nm cut-off for the PCL micelles, 400 nm cut-off for all other micelles) to remove large aggregates. The micelles composed of PCL-PEO (2800–2000), PCL-PEO (6500–5500), PCL-PEO (10 000–5000), PLA-PEO (10 500–5000), PCL-PEO (13 000–5000), PBd-PEO (5500–5000), and PS-PEO (9500–18 000) were denoted as PCL-2800, PCL-6500, PCL-10000, PCL-13000, PLA, PBd, and PS micelles, respectively.

Preparation of PTX-Loaded Micelles: PTX-loaded micelles were prepared by adding PTX during the self-assembly process of the block copolymers. Briefly, 0.1 mL of PTX stock solution (5 mg mL⁻¹) was mixed with 0.1 mL of polymer stock solution (200 mg mL⁻¹, in chloroform) by sonication. Then the mixture was added dropwise to 2.3 mL of MQ water and stirred overnight to remove the organic solvent. A filter with 220 nm cut-off was used to remove the large aggregates in the aqueous system, and SEC using a column (diameter 1 cm, length ≈30 cm) filled with Sephadex G-25 gel was used to remove the unencapsulated PTX molecules. 1 mL of the mixture of PTX and micelles was carefully added into the column, the separation process made use of MQ water as the eluent, and every 1 mL of the eluent was collected as one fraction. The PTX-loaded micelles usually appeared between the 8th to 11th fractions, so four fractions were collected. Then the 4 mL of collected PTX-loaded micelles was concentrated to 1 mL using centrifugation filters.

Radiolabeling with ¹¹¹In(III) and ¹⁷⁷Lu(III): The obtained micelle solution (see 1.2.1) in water was filtered to remove possible aggregates and mixed with HEPES buffer (20 × 10⁻³ M, pH = 7.4) in a volume ratio of 1:1. Next, 50 kBq of ¹¹¹In(III) (the volume was dependent on the decay process and ranged from 5 to 13 μL) was added to 1 mL micelle solution which was subsequently stirred for 30 min. After the reaction, the free ¹¹¹In(III) was removed by SEC. HEPES buffer (10 × 10⁻³ M, pH = 7.4) was used as the eluent. The radiolabeled samples usually appeared between the 8th to 12th fractions, so five fractions in a total volume of 5 mL were collected as the final radiolabeled sample.

¹⁷⁷Lu radiolabeled samples were prepared in the exact same way as the ¹¹¹In samples, i.e., 50 kBq of ¹⁷⁷Lu(III) was used to radiolabel each PCL-PEO micelles sample.

The radiolabeling of PTX-loaded micelles was done in the exact same way as the empty micelles.

Synthesis of In(III) Loaded Micelles: The ¹¹¹In(III) radiolabeled In(III) stock solutions (13.87 × 10⁻³ M) were prepared by adding 60 μL of ¹¹¹In(III) stock solution (0.135 MBq) to 140 μL of nonradioactive indium chloride solution (19.82 × 10⁻³ M, in HCl aqueous solution, pH = 2) (changes of the In³⁺ concentration due to the presence of ¹¹¹In(III) are negligible). In parallel, nonradioactive In(III) stock solutions were prepared by adding 60 μL of HCl aqueous solution (pH = 2) to 140 μL of indium solution with a concentration of 19.82 × 10⁻³ M. The loading process of In(III) was similar with that of ¹¹¹In(III) radiolabeling, i.e., 10 μL of the radiolabeled In(III) solution was added to 1 mL of the micelles in HEPES buffer (10 × 10⁻³ M, pH = 7.4), stirred for half an hour and then the free In(III) was removed by SEC. In this process, HCl solution (pH = 2) was used as the eluent to make sure that indium ions did not precipitate during the separation.

Instruments: DLS instrument consisting of a JDS uniphase 633 nm 35 mW laser, an ALV sp 125 s/w 93 goniometer, a fiber detector, and a Perkin Elmer photo counter was used to obtain the size distributions of the obtained micelles. A Cryo-EM (Jeol JEM 1400) was used to observe the morphology of the micelles and the loading mechanism. FT-IR on a Nicolet 6700 was used to determine possible interaction between the metal ions and functional groups of the micelles. The spectra were recorded in the range from 4000–400 cm⁻¹ with a resolution of 4 cm⁻¹. The automatic Gamma counter (Wallac WIZARD² 2480, Perkin Elmer Technologies) was used to determine the radioactivity of all radiolabeled micelles. An inductively coupled plasma-optical emission spectrometry (ICP-OES) apparatus was applied to detect the loading efficiency of the nonradioactive metals. An HPLC was used to determine the loading efficiency of PTX.

Radiolabeling Efficiency: The formula used to calculate the radiolabeling efficiency (RE) of the micelles was as follow

$$\text{RE (\%)} = \left(\frac{\text{Measured counts per minute of } ^{111}\text{In} / ^{177}\text{Lu encapsulated in micelles}}{\text{Measured counts per minute of initially added activity}} \right) \times 100\% \quad (1)$$

Loading Efficiency of Metal Ions: An ICP-OES facility was applied to determine the loading efficiency of the metal ions without activity. To prepare samples for ICP-OES analysis, 1 mL of the metal-loaded PCL-PEO micelles was mixed with 1 mL aqua regia which was followed by ultrasonication (50 °C, 4 h) to destroy the micellar structure and dissolve the encapsulated metal ions. Then, MQ water (5.0 mL) was added to prepare the final samples for measurement.

Stability Test with DTPA: 0.1 mL of DTPA solution (11 × 10⁻³ M, in 10 × 10⁻³ M HEPES buffer, pH = 7.4) was added to 1 mL of the ¹¹¹In(III) labeled micelles (10 × 10⁻³ M HEPES buffer, pH = 7.4). After being incubated for 1 day, the mixture was passed through an SEC column to separate the free ¹¹¹In-DTPA complex (14th to 17th fractions) and the ¹¹¹In(III) radiolabeled micelles (8th to 12th fractions). The radioactivity left in micelles was measured using the Wallac gamma counter. The DTPA stability test of the other radiolabeled micelles was carried out in the same way.

The Stability Test in FBS Serum: The radiolabeled samples (0.5 mL) were mixed with the same volume of serum and stored in an incubator at 37 °C. After 1 day of incubation, the mixture was separated by a column (diameter 1 cm, length 30 cm) packed with Sepharose 4B gel and HEPES buffer was applied as the eluent. Similar as the operation with SEC column, every 1 mL of the eluent was collected as one fraction. The micelle fractions appeared at fraction 8th to 13th, while the FBS fraction appeared around 17th to 22nd fractions. The activity in each part was measured by the Wallac gamma counter.

In Vivo Biodistribution of ¹¹¹In(III) Radiolabeled Micelles: The radiolabeled micelles for SPECT imaging were prepared by adding 80 MBq of ¹¹¹In(III) to 1 mL of PCL-6500 micelles dispersed in HEPES buffer (10 ×

10^{-3} m) and incubated for 30 min. Subsequently, a PD10 size exclusion column was utilized to remove any free $^{111}\text{In(III)}$ using PBS as the eluent. The fraction containing the largest $^{111}\text{In(III)}$ activity was further used for the in vivo experiments. Before the animal experiments, the stability of the sample in serum was determined by mixing 0.05 mL of the $^{111}\text{In(III)}$ radiolabeled micelles with 0.95 mL of FBS and incubating for 4 h. A Sepharose 4B column was applied to separate the micelles and serum fractions, and the activity in each part was determined by using the Wallac counter.

All animal studies were performed in accordance with the Dutch Law on Animal Experimentation and all protocols were approved by the Animal Research Committee of the University Medical Center Utrecht (AVD11500202011184). The in vivo biodistribution of micelles was carried out using a SPECT/CT scanner (VECTOR⁶/CT, MILabs B.V., The Netherlands). Three healthy C57BL/6 mice of 10 weeks old were used. For the animal studies, 200 μL of $^{111}\text{In(III)}$ radiolabeled PCL-6500 micelles (≈ 10 MBq, dispersed in PBS) was injected into the tail vein of the mice. SPECT/CT image scans were carried out at 1, 24, and 48 h post-injection using a clustered pinhole collimator with 144 pinholes of 0.7 mm diameter each (type HE-HR-M). After SPECT imaging, X-ray CT images were acquired at 50 kV, 0.21 mA, 75 ms exposure time per projection with 720 projections. The animals were anesthetized using a mixture of 2% isoflurane in air. The data were reconstructed using a SROSEM algorithm.^[28,29] with a voxel size of 0.6 mm, 5 iterations and 128 subsets, followed by isotropic 3D Gaussian filtering with 1.5 mm full-width at half-maximum. CT images were reconstructed at 120 μm voxels. SPECT and CT images were spatially registered. The CT data were then used to correct the SPECT image for attenuation.^[30] VOI analysis using the software Pmod 4.2 was performed to quantitatively analyze the data.

Statistical Analysis: All data points referred to the mean \pm standard deviation (SD) and were based on at least three separate experiments ($n = 3$). All statistical tests were performed by Microsoft Excel using student's t -test for comparison between two groups. Statistical significance was represented as $*p \leq 0.05$, $**p \leq 0.01$, $***p \leq 0.001$, and $****p \leq 0.0001$.

Supporting Information

Supporting Information is available from the Wiley Online Library or from the author.

Acknowledgements

This work was financially supported by the China Scholarship Council (grant number 201707040083) and the Delft Health Initiative. The authors also thank Astrid van der Meer and Rene Nouse for managing the radioisotope ordering and transportation. The authors are incredibly grateful to Erik de Blois from Erasmus MC for the supply of ^{111}In and ^{177}Lu . The authors also thank Joep G. Borninkhof for helping with the initial experiments related to the radiolabeling of different polymer micelles.

Conflict of Interest

The authors declare no conflict of interest.

Author Contributions

H.L. performed the experiments and data analysis and drafted the manuscript. R.M.d.K. took most of the Cryo-EM pictures and helped analyze them. A.C.L. helped with the Cryo-EM pictures. E.v.d.H. helped with the preparation of the PBd, PLA, and PS micelles. R.R. and F.J.B. performed and helped analyze the in vivo experiments. R.E. and A.G.D. guided the whole experimental process, analyzed the data, and revised the manuscript.

Data Availability Statement

The data that support the findings of this study are available from the corresponding author upon reasonable request.

Keywords

biodistribution, block copolymer, hydrophobicity, radiolabeling, SPECT imaging

Received: April 13, 2022

Revised: May 24, 2022

Published online:

- [1] L. Salvioni, M. A. Rizzuto, J. A. Bertolini, L. Pandolfi, M. Colombo, D. Prosperi, *Cancers* **2019**, *11*, 1855.
- [2] A. Varela-Moreira, Y. Shi, M. H. A. M. Fens, T. Lammers, W. E. Hennink, R. M. Schiffelers, *Mater. Chem. Front.* **2017**, *1*, 1485.
- [3] C. M. R. Oda, R. S. Fernandes, S. C. de Araujo Lopes, M. C. de Oliveira, V. N. Cardoso, D. M. Santos, A. M. de Castro Pimenta, A. Malachias, R. Paniago, D. M. Townsend, P. M. Colletti, D. Rubello, R. J. Alves, A. L. B. de Barros, E. A. Leite, *Biomed. Pharmacother.* **2017**, *89*, 268.
- [4] H. Maeda, *Adv. Drug Delivery Rev.* **2015**, *91*, 3.
- [5] Y. Miura, A. B. Tsuji, A. Sugyo, H. Sudo, I. Aoki, M. Inubushi, M. Yashiro, K. Hirakawa, H. Cabral, N. Nishiyama, T. Saga, K. Kataoka, *ACS Biomater. Sci. Eng.* **2015**, *1*, 1067.
- [6] J. Sun, L. Sun, J. Li, J. Xu, Z. Wan, Z. Ouyang, L. Liang, S. Li, D. Zeng, *Acta Biomater.* **2018**, *75*, 312.
- [7] B. Hoang, H. Lee, R. M. Reilly, C. Allen, *Mol. Pharmaceutics* **2009**, *6*, 581.
- [8] K. Xiao, Y. Li, J. Luo, J. S. Lee, W. Xiao, A. M. Gonik, R. G. Agarwal, K. S. Lam, *Biomaterials* **2011**, *32*, 3435.
- [9] H. Gao, J. Liu, C. Yang, T. Cheng, L. Chu, H. Xu, A. Meng, S. Fan, L. Shi, J. Liu, *Int. J. Nanomed.* **2013**, *8*, 4229.
- [10] F. Chen, P. A. Ellison, C. M. Lewis, H. Hong, Y. Zhang, S. Shi, R. Hernandez, M. E. Meyerand, T. E. Barnhart, W. Cai, *Angew. Chem., Int. Ed. Engl.* **2013**, *52*, 13319.
- [11] S. Goel, F. Chen, E. B. Ehlerding, W. Cai, *Small* **2014**, *10*, 3825.
- [12] H. Liu, A. C. Laan, J. Plomp, S. R. Parnell, Y. Men, R. M. Dalgliesh, R. Eelkema, A. G. Denkova, *ACS Appl. Polym. Mater.* **2020**, *3*, 968.
- [13] A. C. Laan, C. Santini, L. Jennings, M. de Jong, M. R. Bernsen, A. G. Denkova, *EJNMMI Res.* **2016**, *6*, 12.
- [14] Y. Liu, G. Liu, D. Hnatowich, *Materials* **2010**, *3*, 3204.
- [15] W. Verweij, in *Calculating Chemical Equilibria in Aquatic Systems*, 3rd ed., CHEAQS Next **2014–2017**, P2017, www.cheaqs.eu.
- [16] T. Sato, *J. Therm. Anal. Calorim.* **2005**, *82*, 775.
- [17] A. Leson, V. Filiz, S. Förster, C. Mayer, *Chem. Phys. Lett.* **2007**, *444*, 268.
- [18] F. Ahmed, D. E. Discher, *J. Controlled Release* **2004**, *96*, 37.
- [19] J. Wu, A. Eisenberg, *J. Am. Chem. Soc.* **2006**, *128*, 2880.
- [20] U. R. Dahal, A. Prhashanna, E. E. Dormidontova, *J. Chem. Phys.* **2019**, *150*, 184908.
- [21] D. N. Pandya, N. B. Bhatt, F. Almaguel, S. Rideout-Danner, H. D. Gage, K. K. Solingapuram Sai, T. J. Wadas, *J. Nucl. Med.* **2019**, *60*, 696.
- [22] L. Emmett, K. Willowson, J. Violet, J. Shin, A. Blanksby, J. Lee, *J. Med. Radiat. Sci.* **2017**, *64*, 52.
- [23] V. Kumar, V. Mundra, Y. Peng, Y. Wang, C. Tan, R. I. Mahato, *Theranostics* **2018**, *8*, 4033.

- [24] L. Cheng, S. Shen, D. Jiang, Q. Jin, P. A. Ellison, E. B. Ehlerding, S. Goel, G. Song, P. Huang, T. E. Barnhart, Z. Liu, W. Cai, *ACS Nano* **2017**, *11*, 12193.
- [25] L. Tian, X. Yi, Z. Dong, J. Xu, C. Liang, Y. Chao, Y. Wang, K. Yang, Z. Liu, *ACS Nano* **2018**, *12*, 11541.
- [26] M. Cachovan, A. H. Vija, J. Hornegger, T. Kuwert, *EJNMMI Res.* **2013**, *3*, 45.
- [27] K. McLarty, B. Cornelissen, Z. Cai, D. A. Scollard, D. L. Costantini, S. J. Done, R. M. Reilly, *J. Nucl. Med.* **2009**, *50*, 1340.
- [28] P. E. B. Vaissier, F. J. Beekman, M. C. Goorden, *Phys. Med. Biol.* **2016**, *61*, 4300.
- [29] M. C. Goorden, C. Kamphuis, R. M. Ramakers, F. J. Beekman, *Phys. Med. Biol.* **2020**, *65*, 105014.
- [30] C. Wu, J. R. De Jong, H. A. Gratama van Andel, F. van der Have, B. Vastenhouw, P. Laverman, O. C. Boerman, R. A. J. O. Dierckx, F. J. Beekman, *Phys. Med. Biol.* **2011**, *56*, N183.